Analysis of Magnetic Coupling in Coaxial CRLH-TLs

Ch. Neumaier[1,2], M. Lorenz[1], N. Spaeth[1], K. Numssen[1] and E. Biebl[2]

[1]Spinner GmbH
Aiblinger Str. 30, D-83620, Feldkirchen-Westerham, Germany
email: christoph.neumaier@spinner-group.com
[2]Fachgebiet Höchstfrequenztechnik, Technische Universität München
Arcisstr. 21, D-80290, München, Germany
email: biebl@tum.de

Abstract

The aim of this investigation are strongly magnetically coupled coaxial CRLH-TLs. For the proper prediction of the dispersion diagram, multiple coupling coefficients have to be taken into account. In this first step, we use the left-handed branch from fullwave calculations for the extraction of self-inductance, as well as mutual inductances for different configurations of our coaxial setup.

1. Introduction

The theory of composite right/left-handed transmission lines (CRLH-TLs) is already a well established tool for the design of 1D metamaterials [1]. These structures exhibit a left-handed branch which enables the engineer to create small designs for devices and structures depending on a well defined electrical length. In most cases, microstrip is used as the base technology, because it is cheap and processing times are low. At elevated power levels (typ. $>\sim 300W$), however, microstrip designs are not applicable anymore. Therefore, we have transferred the CRLH-TL concept to coaxial rigid lines as base technology (cf. Fig. 1(a)). Starting with an implementation according to Fig. 1(a), we find that magnetic coupling between adjacent posts affects significantly the resulting dispersion (see Fig. 1(b)) [2], which is particularly the case for $p < D$.

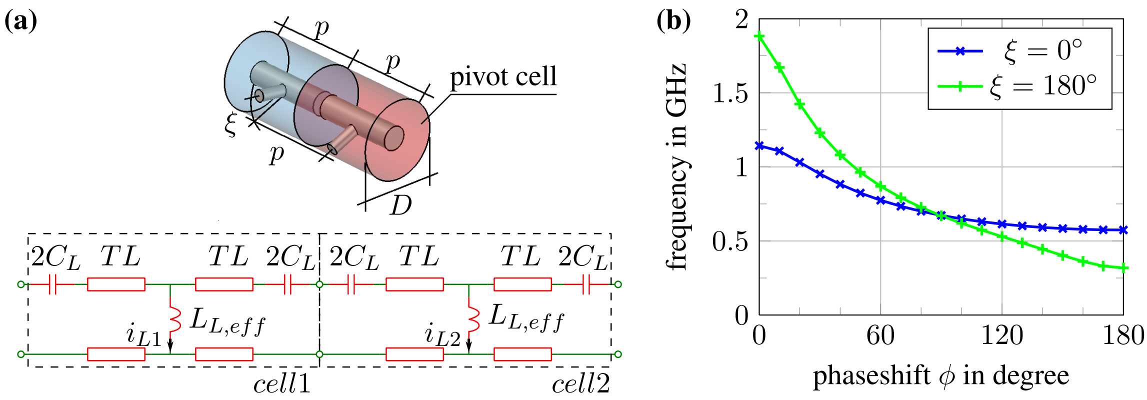

Fig. 1: Schematics. (a) Two unit cells in a row. Two consecutive posts have a distance of p along the direction of the line and are twisted against each other by the angle ξ. (b) Dispersion diagram for $\xi \in \{0°; 180°\}$. Owing to coupling effects, the bandwidth differs by a factor of 2.7.

2. Analysis

The CRLH-TL to be analyzed consists of a conventional coaxial line (outer conductor's diameter D, characteristic impedance Z_R and unit cell's length p) with two alterations (cf. Fig. 1(a)). The first one is the interrupted inner conductor that generates the left-handed capacitance C_L. The second one are the posts in the middle of the unit cell[1] connecting the inner conductor with the outer conductor and representing the left-handed inductance L_L. Since we have abandoned the planar geometry, we attain an additional degree of freedom, which is the twist angle ξ between two adjacent posts. The two cells shown in Fig. 1(a) form the unit cell of a super lattice [3]. From the two cells, we derived an equivalent circuit, which will be used for the extraction of the coupling coefficients in a periodic system (cf. Fig. 1(a) bottom).
Owing to the repeated outline, the current i_{L1} in the post of the pivot cell is related to the current i_{L2} in the post of its neighboring cell by: $i_{L1} = e^{j\phi} i_{L2}$ (periodic boundary conditions, phase shift ϕ). This yields an effective inductance which is dependent on ϕ:

$$L_{L,eff}(\phi) = L_{L,00} + \sum_{k=-\infty}^{+\infty} L_{L,0k} e^{j\phi k} \tag{1}$$

where $L_{L,00}$ is the self-inductance and $L_{L,0k}$ are the mutual inductances. In addition, with the help of a $Bloch - Floquet$ analysis, it is possible to compute the dispersion diagram using the ABCD matrix of one single unit cell as a reference model:

$$\cos(\phi) = A = \frac{2\omega \sin(2\omega\tau) C_L Z_R^2 + [4\omega^2 \cos(2\omega\tau) C_L L_L - \cos(2\omega\tau) - 1] Z_R + 2\omega \sin(2\omega\tau) L_L}{4\omega^2 C_L L_L Z_R} \tag{2}$$

with $L_L \equiv L_{L,eff}(\phi)$, $\tau = \frac{p}{2c_0}$, where c_0: speed of light and $\phi = \beta p$: phase shift over one unit cell length. By rearranging this equation for $L_{L,eff}$:

$$L_{L,eff}(\phi) = \frac{2\omega \sin(2\omega\tau) C_L Z_R^2 + [-\cos(2\omega\tau) - 1] Z_R}{[4\omega^2 \cos(\phi) - 4\omega^2 \cos(2\omega\tau)] C_L Z_R - 2\omega \sin(2\omega\tau)} \tag{3}$$

we may now extract the effective $L_{L,eff}(\phi)$ with the help of a fullwave simulation of our unit cells, because the left-handed branch in the dispersion pinpoints an angular frequency $\omega = 2\pi f$ for a given ϕ. Since the fullwave simulation outputs the left-handed branch discretely sampled over ϕ, the coefficients for a finite series may be extracted with the help of an FFT or DCT.

3. First results

In this section we show first results of the extraction method applied to our structure. The method is supposed to extract the coefficients for a later prediction of the dispersion without a time consuming fullwave eigenmode calculation [4], [5].
After the calculation of the eigenmodes in a fullwave simulation for the two cell model, the effective dispersion for one unit cell is mapped by unfolding the left-handed branch and rescaling the ϕ axis for an interval of $0° \leq \phi \leq 180°$. This dispersion is then used in order to extract $L_{L,eff}$. We mirror $L_{L,eff}$ along $\phi = 180°$ in order to get a continuous even function which will lead to a real valued spectrum.

3.1 Dependence on the twist angle ξ

In the scope of this section we confine ourselves to the case of parallel and anti-parallel posts, i.e. $\xi \in \{0°; 180°\}$. When comparing $L_{L,eff}$, one may notice that for $\xi = 0°$ the maximum is at $\phi = 0°$, whilst

[1] In the scope of this paper, only symmetric and lossless unit cells are dealt with.

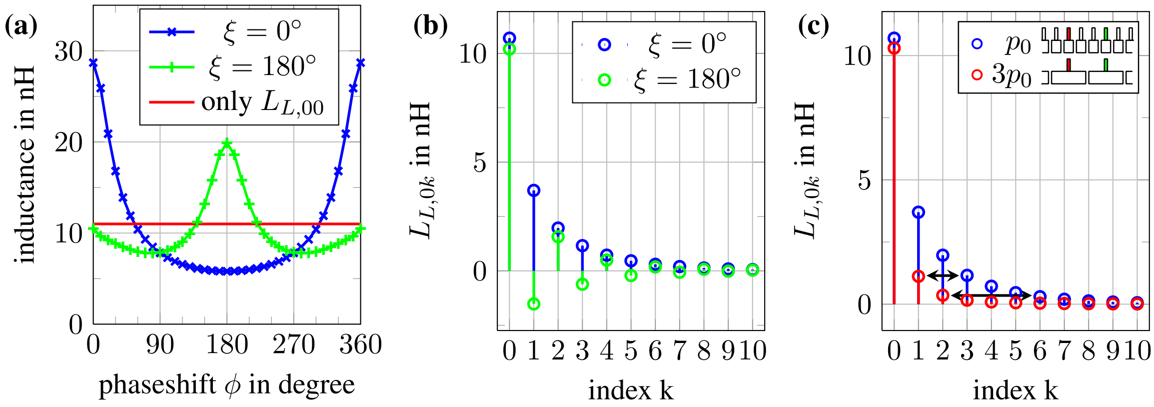

Fig. 2: First results. (a) $L_{L,eff}(\phi)$ for $\xi \in \{0°; 180°\}$ and self-inductance. (b) $L_{L,0k}$ for $\xi \in \{0°, 180°\}$. For $\xi = 180°$ an alternation of the coupling coefficients may be observed. The self-inductance $L_{L,00}$ is extracted at good fidelity (compare value for $k = 0$ with the extracted value from S-parameter simulation in (a)). (c) $L_{L,0k}$ for $p \in \{p_0; 3p_0\}$. The corresponding coefficients are marked by arrows.

for $\xi = 180°$, the maximum is at $\phi = 180°$. Since C_L and C_R, which are the constituent parts (apart from L_L) in the description of left-handed and shunt resonances according to [1], and since these two parameters are not changed for the cases $\xi \in \{0°; 180°\}$, this leads to enlarged left-handed branches for $\xi = 180°$ in comparison to $\xi = 0°$ (c.f. Fig. 1(b) & Fig. 2(a)). Due to anti-parallel orientation of the posts for $\xi = 180°$, one expects the mutual inductance to be negative. This is proven in Fig. 2(b), where the mutual inductances turn out to be negative for odd indices.

3.2 Dependence on the unit cell length p

In this part, we only changed the unit cell length, thus leaving self-inductance, Z_R, C_L and $\xi = 0°$ all the same. When the case for $p = p_0$ is compared with the case where $p = 3p_0$, one recognizes that the distance between the post of the pivot cell and the post under consideration is the cause for the approximately exponential decay of $L_{L,0k}$. This leads to nearly equal coefficients: $L_{L,0(m)}\,|_{p=3p_0} \approx L_{L,0(3m)}\,|_{p=p_0}$, $m \in N$ (see Fig. 2(c)).

4. Conclusion

In this paper we have described the influence of higher order magnetic coupling coefficients on the dispersion diagram of a coaxial CRLH-TL implementation. We have shown how to extract the different coefficients from a dispersion diagram, obtained by a fullwave simulation, in order to be able to predict the dispersion with high confidence.

References

[1] C. Caloz and T. Itoh, *Electromagnetic Metamaterials,* Hoboken(New Jersey), USA: Wiley & Sons, 2006.
[2] R.R.A. Syms et al., Higher order interactions in magneto-inductive waveguides, *Metamaterials,* vol. 1, pp. 44-51, 2007.
[3] L. Brillouin, *Wave Propagation in Periodic Structures,* New York, USA: McGraw-Hill Book Company, 1946.
[4] L. Solymar and E. Shamonina, *Waves in Metamaterials,* Reprint 2010, Oxford, England: Oxford University Press, 2010.
[5] O. Zhuromskyy et al., Slow waves on magnetic metamaterials and on chains of plasmonic nanoparticles: Driven solutions in the presence of retardation, *Journal of Applied Physics,* vol. 106, p.104908, 2009.